





Cite this: *Sens. Diagn.*, 2023, 2, 1553

## EXPAR and Au–Ag mushroom-shaped SERS probe assisted detection of exosomal miR-375 in prostate cancer

Chenxiao Tang,<sup>†a</sup> Zhipeng Huang, <sup>†a</sup> Huixiang Li,<sup>a</sup> Ren Zhang, <sup>a</sup> Guopeng Yu,<sup>c</sup> Jilie Kong,<sup>a</sup> Hui Chen <sup>\*a</sup> and Wenhao Weng<sup>\*b</sup>

Exosomes carry abundant bioactive substances from parent cells, which contain tremendous amounts of proteins and nucleic acids and can be used as important diagnostic markers of diseases. In this work, we developed an EXPAR and Au–Ag mushroom-shaped SERS probe assisted strategy for the detection of exosomal miR-375 in prostate cancer. The EXPAR was triggered by the target miRNA and the amplification products were detected by the Au–Ag mushroom-shaped SERS tag, thus realizing the sensitive detection of miRNA. Prostate-specific membrane antigen (PSMA) positive exosomes captured by magnetic beads were released and lysed. This method was used to detect the concentration of miR-375 in PSMA-positive exosomes. The limit of detection was 10 fM. This method was also successfully employed to distinguish clinical serum samples from healthy people and prostate cancer patients, and has great potential application in the clinical diagnosis of prostate cancer.

Received 10th June 2023,  
Accepted 18th September 2023

DOI: 10.1039/d3sd00145h

[rsc.li/sensors](https://rsc.li/sensors)

## Introduction

miRNAs are a class of short endogenous non-coding RNA with 18–24 bp.<sup>1</sup> It has been established that miRNAs control gene expression and are essential for cell proliferation, growth, and apoptosis. Therefore, miRNAs can be employed as biomarkers for the diagnosis and prognosis of diseases.<sup>2,3</sup>

Exosomes are tiny vesicles with a phospholipid bilayer membrane secreted by almost all living cells.<sup>4</sup> Researchers have discovered that exosomes contain many molecules, including proteins and nucleic acids, and that their phospholipid bilayer membrane structure shields the molecules inside from enzymes and other environmental factors.<sup>5</sup> Non-coding RNAs, such as miRNA, lncRNA, tsRNA and circRNA, are also found in exosomes and are involved in a number of clinical processes.<sup>6,7</sup> Exosomal miRNA is the most extensively researched non-coding RNA. It is possible to employ tumor-derived exosomal miRNAs as biomarkers for the diagnosis, monitoring, and prognosis of clinical diseases.<sup>8</sup> Exosomal miRNAs offer two benefits over conventional tissue biopsies in terms of being

suitable biomarkers: (1) they can be persistently present in body fluids, and (2) they are simple to get and may be collected non-invasively from blood, urine, and saliva.<sup>9</sup> Exosomal miR-1290 and miR-375 in plasma exosomes are predicted to be utilized as biomarkers for the diagnosis and prognosis of desmoresistant prostate cancer.<sup>10</sup> Exosomal miR-375 in serum samples also showed an accuracy of 85% for the detection of estrogen receptor-positive breast cancer at early stages using a thermophoretic sensor implemented with nanoflakes.<sup>11</sup> The Zeng group developed a one-step, one-pot isothermal miRNA assay termed “Endonucleolytically eXponentiated Rolling circle Amplification with the dual-functional CRISPR-Cas12a” (EXTRA-CRISPR) to detect miRNAs (miR-21, miR-196a, miR-451a, and miR-1246) in plasma extracellular vesicles, which can define a potent EV miRNA signature for the diagnosis of pancreatic cancer.<sup>12</sup> There is an urgent need to develop a highly sensitive test for exosomal miRNA identification in microsamples because current techniques have problems with low abundance, short duration, large sample requirements, and high similarity of family member sequences.<sup>11</sup>

Exponential isothermal amplification (EXPAR) is activated by specific DNA primers, followed by a quick (30 min) amplification process mediated by polymerase and endonuclease to produce significant amounts of the target molecule.<sup>13,14</sup> Due to its high amplification efficiency ( $10^6$ – $10^8$ ) and straightforward operational design, EXPAR has been incorporated into the amplified detection of nucleic acids, proteins, enzyme activities, metal ions, and cells.<sup>15</sup> The miRNAs extracted from exosomes were quantitatively detected based on

<sup>a</sup> Department of Chemistry, Fudan University, Shanghai, 200438, China.  
E-mail: [chenhui@fudan.edu.cn](mailto:chenhui@fudan.edu.cn)

<sup>b</sup> Department of clinical laboratory, Children's hospital of Shanghai, Shanghai Jiaotong University School of Medicine, Shanghai 200011, China.  
E-mail: [wengwenhao@shchildren.com.cn](mailto:wengwenhao@shchildren.com.cn)

<sup>c</sup> Department of Urology, Shanghai Ninth People's Hospital, Shanghai Jiaotong University School of Medicine, Shanghai 200011, China

<sup>†</sup> These authors contributed equally to this work.



the on-chip capture of exosomes, exponential amplification reaction (EXPAR) of miRNA and fluorescence detection.<sup>16</sup>

Surface-Enhanced Raman Scattering (SERS) has attracted tremendous attention for the detection of biomolecules with low concentrations because of its fast response and superior sensitivity. The most common mechanism to improve the sensitivity of SERS sensors is to create “hot spots” structures resulting in a local electromagnetic field enhancement. A uniform plasmonic head-flocked gold nanopillar substrate has been developed for the quantitative and specific detection of exosomal miRNAs, which generates multiple hotspots and enables hybridization between miRNAs and locked nucleic acid probes.<sup>17</sup> In addition to “hot spots”, the Cai group designed a close-packed and ordered Au octahedral array as a sensing platform for the quantitative determination of let-7a miRNAs in MCF-7 cell derived exosomes, which produced “hot surfaces” rather than “hot spots” and greatly improved the detection sensitivity and uniformity.<sup>18</sup> Metal nanostructures with a tunable plasmonic gap are useful for SERS detection due to the field-enhanced transverse cavity plasmon mode excited in the narrow face-to-face gaps as Fabry-Pérot-like resonances.<sup>19,20</sup> Therefore, Au dual-gap mushroom-shaped nanodumbbells (AuDGNs) within a single particle have been designed and synthesized for the label free on-particle SERS detection of DNA with high sensitivity.<sup>20</sup> Furthermore, DNA-mediated gold-silver nanomushrooms with interior nanogaps (1–2 nm) were synthesized and the SERS enhancement factors reached about  $10^9$  orders of magnitude, where the DNA involved in the nanostructures can act as not only gap DNA (mediated DNA) but also probe DNA (hybridized DNA).<sup>21</sup> Therefore, the Au-Ag mushroom-shaped SERS probes have high SERS enhancement and bio-molecular recognition abilities.

In order to improve the detection sensitivity, in this work, signal amplification and enhancement strategy was integrated, where the DNA probe mediated the formation of the mushroom-shaped Au-Ag SERS probe and hybridized with the EXPAR amplicons triggered by target miRNA. Finally, we integrated SERS probes in the form of mushrooms with EXPAR amplification for miR-375 detection in prostate cancer exosomes.

## Experiments and methods

### 1. Materials and reagents

Vent (exo-) DNA polymerase, Nt.BstNBI nicking enzyme, NEBuffer (100 mM NaCl, 50 mM Tris-HCl, 10 mM MgCl<sub>2</sub>, 100 µg mL<sup>-1</sup> recombinant albumin, pH 7.9), ThermoPol Buffer (20 mM Tris-HCl, 10 mM (NH<sub>4</sub>)<sub>2</sub>SO<sub>4</sub>, 10 mM KCl, 2 mM MgSO<sub>4</sub>, 0.1% Triton® X-100, pH 8.8) and DEPC water were purchased from New England BioLabs. Phosphate-buffer (PB, 0.1 M NaH<sub>2</sub>PO<sub>4</sub> + 0.1 M Na<sub>2</sub>HPO<sub>4</sub>, pH = 7.2–7.4.) was prepared. Human prostate cancer cells (LNCaP), human normal prostate epithelial cells (RWPE-1) and human breast cancer cells (MCF-7) were purchased from Shanghai Zeiba Biotechnology Co, China. A Trizol total RNA extraction kit was purchased from Shanghai Bioengineering Co, China. An

**Table 1** The nucleic acid sequences used in this work

Name	Sequences(5' to 3')
Template-375	GATGCTCACTGACTGCTAGGATGGTATGACT CGATGCTCACTGACTGCTAGGATGGTATGA CTCTCGCGCGAGCCGAACGAACAAAA-P
Trigger-375	CATCCTAGCAGTCAGTGAGCATC
Capture probe 1 (CP1)	CTGCTAGGATGTTTTTTTTT-SH
Capture probe 2 (CP2)	Biotin-TTTTTT TTTGATGCTCACTGA
miR-375	UUUGUUCGUUCGGCUCGCGUGA
Amino-modified PSMA aptamer	GCGTTTTTCGCTTTTTCGCTTTTGGGTTCATCTG CTTACGATAGCAATGCTTTTTTTTTTTT-NH <sub>2</sub>

RNase inhibitor and dNTP mixture was purchased from the APE×BIO company, USA. Polyvinyl pyrrolidone (PVP) K30 and *p*-ATP (4-aminothiophenol) were purchased from Sigma-Aldrich, Shanghai, China. Streptavidin-modified magnetic beads (750 nm, 10 mg mL<sup>-1</sup>) were purchased from Shanghai Carfax Biomedical Technology Co, China. Tris(2-carboxyethyl) phosphine hydrochloride (TCEP) and all oligonucleotides were synthesized by Sangon Biotech Co. Ltd., China and their sequences are shown in Table 1. The PSMA aptamers were designed according to previous work.<sup>22</sup>

### 2. Instruments

A LineGene 9600 real-time fluorescence quantitative PCR instrument (Hangzhou Bo Ri Technology Co., Ltd., China) was used for fluorescence signal acquisition of EXPAR amplification reactions. A vertical electrophoresis tank (Bio-RAD Mini PROTEAN Tetra Cell), an electrophoresis instrument (Tanon EPS 300, Tanon Company, China) and a digital gel processing system (Tanon 4100, Tanon Company, China) were used to characterize the EXPAR amplification results. The morphology of Au-Ag mushroom-shaped SERS probes were characterized using a HT7700 transmission electron microscope (Hitachi, Japan) at an accelerating voltage of 120 kV. A Horiba Jobin Yvon XploRA type micro Raman spectrometer was used for Raman spectroscopy signal acquisition with an excitation light wavelength of 785 nm.

### 3. Preparation of the DNA aptamer and Raman probe molecule co-modified AuNPs

Au nanoparticles of 40 nm were synthesized using a previously reported procedure.<sup>23</sup> To cleave the disulfide bond, the thiolated DNA (CP1) was reduced with TCEP as in the reference.<sup>24</sup> Firstly, CP1 was dissolved in 400 µL 10 mM TCEP at room temperature for 1 h, and then 50 µL 3 M sodium acetate (pH = 5.2) and 1.5 mL ethanol was added to the solution successively and vortexed. The mixture was placed in a -80 °C refrigerator for 20 min and then centrifuged for 10 min at 12 000 rpm. The precipitate was redissolved with the appropriate amount of RNase-free water. Next, 200 µL AuNPs were added to 10 µL CP1 (10 µM) and the reaction was carried out at room temperature for 12 h. After the reaction,



0.2 M PB was added to a final concentration of 10 mM for 30 min, and the reaction was carried out overnight at room temperature by adding 2 M sodium nitrate solution three times at a 1 h interval to a final concentration of 0.1 M. After centrifugation at 7500 rpm for 15 min, the excess DNA strand was removed by washing for three times and the precipitate was finally dissolved in 200  $\mu$ L of 10 mM PB. The AuNPs (200  $\mu$ L) obtained by centrifugation in the previous step were mixed with 20  $\mu$ L of 5 mM *p*-ATP solution and reacted in a constant temperature shaker (37  $^{\circ}$ C) for 2 h. The precipitate was centrifuged at 7500 rpm for 15 min, washed three times to remove excess Raman signal molecules (*p*-ATP), and finally resuspended in 200  $\mu$ L of 10 mM PB solution.

#### 4. Preparation and characterization of the Au-Ag mushroom-shaped SERS probe

100  $\mu$ L of AuNPs co-modified with DNA aptamer and Raman probe molecules were added to 200  $\mu$ L of 1% PVP and mixed well. And then 30  $\mu$ L of 20 mg mL<sup>-1</sup> sodium ascorbate solution was added, shaken 8 times, and 30  $\mu$ L of 1 mM silver nitrate solution was quickly added, vortex shaken for 1 min, and left at room temperature for 30 min. After that, the AuNPs were washed three times with 10 mM PB solution and resuspended in 50  $\mu$ L PB solution. At last, 3  $\mu$ L of the SERS probe was added dropwise onto the copper network, dried and then characterized by TEM.

#### 5. EXPAR reaction

The EXPAR amplification reaction consists of reaction mixture A, which contains miR-375 dilution, amplification template (template-375), dNTPs, RNase inhibitor, NEBuffer and DEPC water, and reaction mixture B, which contains Vent (exo-) DNA polymerase (2000 units mL<sup>-1</sup>), Nt.BstNBI cutase (1000 units mL<sup>-1</sup>), Nt. ThermoPol Buffer, DEPC water and SYBR Green I fluorescent dye. Reaction mixture A and reaction mixture B were mixed and put into a real-time quantitative fluorescence PCR instrument, and the reaction temperature was set at 55  $^{\circ}$ C, and the fluorescence signal was collected every 30 s interval. The EXPAR reaction system for the fluorescence PCR instrument consisted of 1  $\mu$ L miR-375 dilution, 1  $\mu$ L template-375 (500 nM), 1  $\mu$ L dNTPs (2.5 mM), 0.2  $\mu$ L RNase inhibitor, 0.5  $\mu$ L NEBuffer, 0.4  $\mu$ L Nt.BstNBIase, 0.25  $\mu$ L Vent (exo-) DNA polymerase, 1  $\mu$ L ThermoPol Buffer, 1  $\mu$ L SYBR Green I fluorescent dye and 3.65  $\mu$ L DEPC water. 1  $\mu$ L SYBR Green I fluorochrome was replaced with 1  $\mu$ L DEPC water when the EXPAR reaction system was used for the following SERS assay.

#### 6. Modification of magnetic beads with CP2 and SERS detection of miRNA using Au-Ag mushroom-shaped SERS probe

200  $\mu$ L of 10 mg mL<sup>-1</sup> streptavidin-modified magnetic beads were firstly washed three times with 1 mL of 1 $\times$ B&W Buffer (5 mM Tris-HCl, pH = 7.5, 0.5 mM EDTA and 1 M NaCl) and then resuspended with 400  $\mu$ L of 2 $\times$ B&W Buffer. 400  $\mu$ L of 5

$\mu$ M CP2 strands were added and left at room temperature for 30 min. The supernatant was removed after magnetic separation. After that, the CP2-modified magnetic beads were washed three times with 500  $\mu$ L of 1 $\times$ B&W Buffer, and finally dissolved in 200  $\mu$ L of PBS solution.

10  $\mu$ L of EXPAR amplification product was added to 10  $\mu$ L of washed magnetic beads (5 mg mL<sup>-1</sup>), and reacted at 37  $^{\circ}$ C for 90 min. After magnetic separation and washing three times, 10  $\mu$ L of Au-Ag mushroom-shaped SERS probe was added, reacted at 37  $^{\circ}$ C for 60 min, magnetically separated and washed three times, and finally was dissolved in 10  $\mu$ L of water. 3  $\mu$ L of the reacted mixture was taken, dripped on the silicon wafer and dried at room temperature for measurement. The parameters of the laser confocal Raman instrument detection were set as follows: the excitation light (785 nm laser) is selected, the signal acquisition time is 10 s, and the inscribed line density is 600 lines per mm of grating.

#### 7. The capture of exosomes from clinical serum samples

The PSMA aptamer modified MBs were prepared by standard protocols suggested by the manufacturer. Briefly, 200  $\mu$ L of 10 mg mL<sup>-1</sup> MBs were washed twice with 500  $\mu$ L MEST (10 mM MES, pH = 6, 0.05% Tween 20), and 200  $\mu$ L of 5 mg mL<sup>-1</sup> EDC and 200  $\mu$ L of 5 mg mL<sup>-1</sup> NHS were added to the solution to activate -COOH groups on the MBs. After that, 10  $\mu$ L of 100  $\mu$ M amino-modified PSMA aptamer was added to the activated MB solution and allowed to react for 3 h at 37  $^{\circ}$ C. Finally, the MBs were blocked by 1% BSA for 30 min at 37  $^{\circ}$ C and then washed with PBST for 5 times. The MBs were dispersed in PBST and stored at 4  $^{\circ}$ C.

The serum samples were provided by Shanghai Ninth People's Hospital, China. 10 serum samples from patients and 9 serum samples from healthy people were detected by the proposed assay. Written informed consent was obtained at the beginning of the research. All experiments on the clinical serum samples were approved by the Medical Research Ethics Committee, Shanghai Ninth People's Hospital, Shanghai, China. The samples were collected and centrifuged at 3000 rpm for 5 min, and the supernatant was filtered through a 0.22  $\mu$ m filter membrane.

10  $\mu$ L clinical serum samples was added and incubated with 10  $\mu$ L of PSMA aptamer modified MBs for 0.5 h at 37  $^{\circ}$ C with gentle shaking. And then the mixture was magnetically separated. The exosome captured MBs in the bottom of EP tube were used for the detection of internal miRNA in exosomes.

#### 8. The release and detection of miR-375 from PSMA-positive exosomes in clinical serum samples

The exosome captured MBs were added to an enzymatic digestion reaction system mediated by DNase I, which consisted of 2  $\mu$ L DNase I, 2  $\mu$ L 10 $\times$  reaction buffer (100 mM Tris-HCl, 25 mM MgCl<sub>2</sub>, 1 mM CaCl<sub>2</sub>, pH 7.5) and 16  $\mu$ L HEPES buffer, and the reaction was carried out at 37  $^{\circ}$ C. After magnetic separation, the supernatant was extracted from the released exosomes using the Trizol Total RNA Extraction Kit, and then the miR-375 of PSMA-positive exosomes was





detected according to the method in the Experiments section part 6. The data were processed using the GraphPad Prism 8 software, and the difference with  $p < 0.05$  was considered statistically significant.

## Results and discussion

### 1. The detection principle of exosomal miRNA

The principle of EXPAR-SERS-based exosomal miR-375 detection is shown in Scheme 1, which consists of two key steps: EXPAR amplification and SERS detection.

**EXPAR amplification:** the template for EXPAR (template-375) is constructed as A'N'A'N'B', where B' stands for the miR-375 recognition site and N' includes the complementary site that was cut by the Nt.BstNBI cutter enzyme. When the target miR-375 is present, template-375 can bind to the target to form a double-stranded recognition sequence and polymerize along the 3' end of the miR-375 in the presence of Vent (exo-) DNA polymerase and dNTPs to produce dsDNA. This dsDNA contains the cleavage recognition site of the Nt.BstNBI incision enzyme site (5'-GAGTC-3'). Continuous polymerization, cleavage, and strand substitution produce the B and AN strands (the complementary strand of B' and A'N'). Another cycle is started when the newly created AN carrying the target sequence hybridizes with template-375. Therefore, one target miRNA produces several A strands (named as trigger DNA in the following SERS detection step) and amplifies the detection signal.

**SERS assay.** When the trigger DNA (the amplification product of EXPAR) is present, the trigger DNA strand hybridizes with CP2 modified on magnetic beads and the other end hybridizes with CP1 on the mushroom-shaped SERS probe. The final sandwich structure of magnetic beads/trigger DNA/SERS probe was formed, and the highly sensitive detection of miR-375 was accomplished by Au-Ag mushroom-shaped SERS probes assisted with EXPAR amplification.

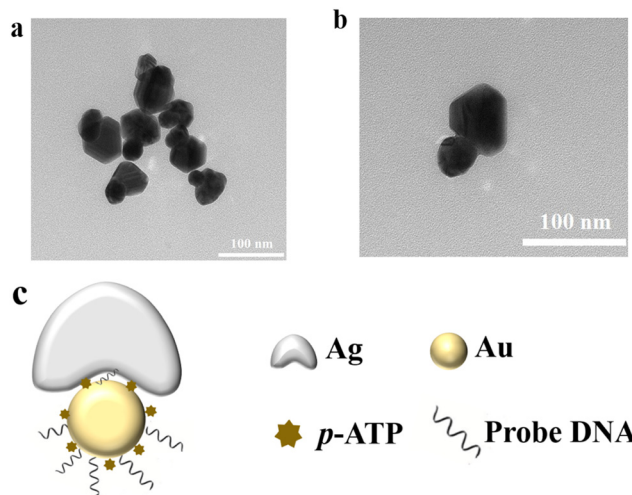


Fig. 1 (a) and (b) TEM characterization of the Au-Ag mushroom-shaped SERS probe, and (c) sketch of the SERS probe.

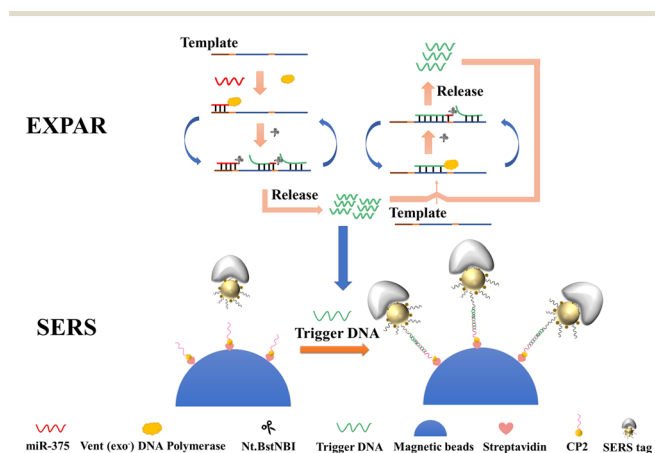
### 2. Characterization of the Au-Ag mushroom-shaped SERS probes

The mushroom-shaped SERS probes with a high SERS enhancement factor were prepared on 40 nm AuNPs surface. The silver was first formed in the DNA layer, then growing as the mushroom cap with interior DNA nanogaps. The density of CP1 coverage on the AuNPs highly influenced the formation of the mushroom-shaped SERS probe, since the CP1 DNA layer might block the direct deposition of silver onto the gold surface.<sup>25</sup> The Au-Ag mushroom-shaped nanostructures were then characterized by TEM, as shown in Fig. 1. Almost all probes were in the shape of a mushroom with uniform interior voids, and not a shell structure. The nanogaps caused the increase of the surface electromagnetic field, resulting in increased intensities of SERS signals.<sup>25</sup> The semi-coated silver is present on the surface of AuNPs and is exposed to free nucleic acids, allowing the mushroom-shaped SERS probe to hybridize complementarily to the target nucleic acids.

### 3. Verification of EXPAR and Au-Ag mushroom-shaped SERS probe assisted detection of miR-375

The EXPAR reaction was conducted on a real-time fluorescence quantitative PCR instrument and the change of fluorescence in the reaction was recorded as shown in Fig. 2(a) with the inset displaying the PolyAcrylamide Gel Electrophoresis (PAGE) of the EXPAR products. When the target miR-375 is present, the reaction results in a considerable increase in the fluorescence signal. Otherwise, the increase in fluorescence intensity when the target is absent is negligible. As shown in the inset PAGE image, without target miR-375 (lane 1), there is only a band of template DNA but no such band of trigger DNA, which indicated that EXPAR didn't take place. In contrast, when miR-375 was added, which allows the EXPAR reaction to proceed properly, the desired trigger DNA band (lane 2) was seen in the PAGE.

Besides, we synthesized the trigger DNA strand artificially and analyzed the EXPAR amplification products by PAGE



Scheme 1 Schematic diagram of exosome miR-375 detection in prostate cancer cells based on EXPAR and mushroom-shaped SERS probes.



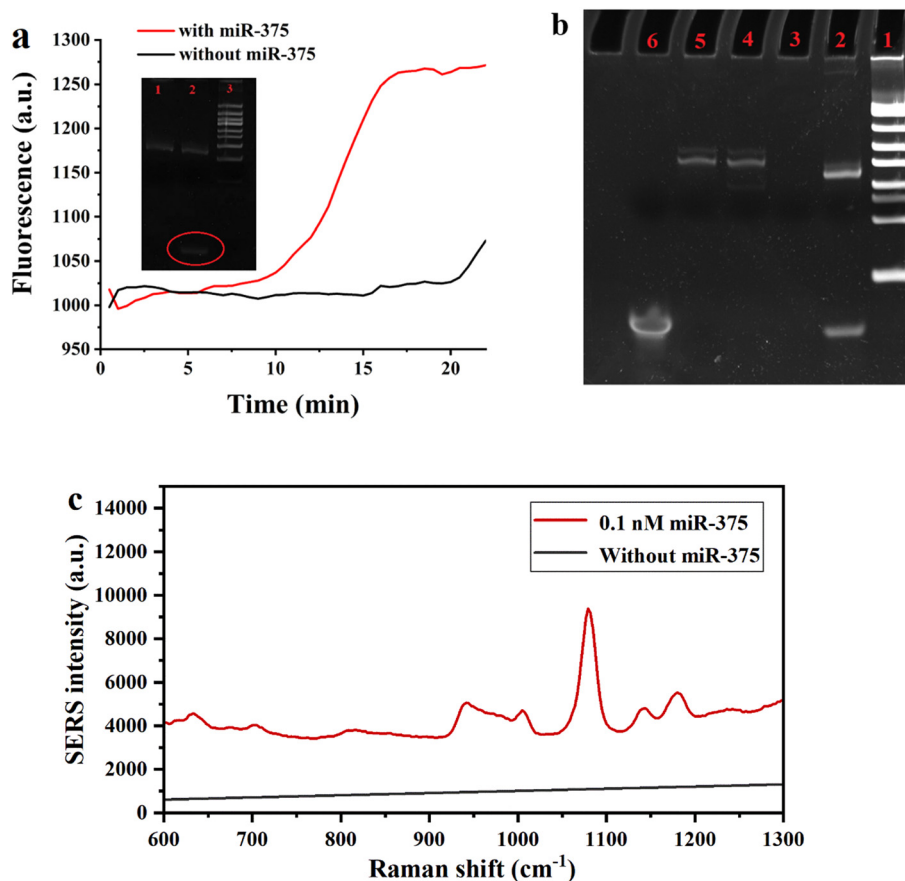


**Fig. 2** (a) Real-time fluorescence intensity curves of EXPAR reactions; the red curve is the miR-375 experimental group and the black curve is the blank control group. The insets indicate the corresponding PAGE results: lane 1: no miR-375; lane 2: 100 nM miR-375 EXPAR amplification product, with 1000 units  $\text{ml}^{-1}$  Nt.BstNBI and 200 units  $\text{ml}^{-1}$  Vent (exo-) DNA enzyme; lane 3: DNA ladder, (b) PAGE characterization plots of EXPAR products: lane 1: 25 bp DNA ladder; lane 2: EXPAR amplification product; lane 3: 0.1 nM miR-375 + 1000 units  $\text{ml}^{-1}$  Nt.BstNBI + 200 units  $\text{ml}^{-1}$  Vent (exo-) DNA enzyme; lane 4: 0.1 nM miR-375 + template-375 + 200 units  $\text{ml}^{-1}$  Vent (exo-) DNA enzyme; lane 5: 0.1 nM miR-375 + template-375 + 1000 units  $\text{ml}^{-1}$  Nt.BstNBI; lane 6: trigger DNA. (c) SERS spectra with and without 0.1 nM miR-375. The parameters of the laser confocal Raman instrument detection were set as follows: the excitation light (785 nm laser) is selected, the signal acquisition time is 10 s, and the inscribed line density is 600 lines per mm of grating.

under different circumstances to confirm that trigger DNA was produced by EXPAR amplification. As shown in Fig. 2b,

lane 6 represents the artificially synthesized trigger DNA and lane 2 represents the EXPAR amplification product band.

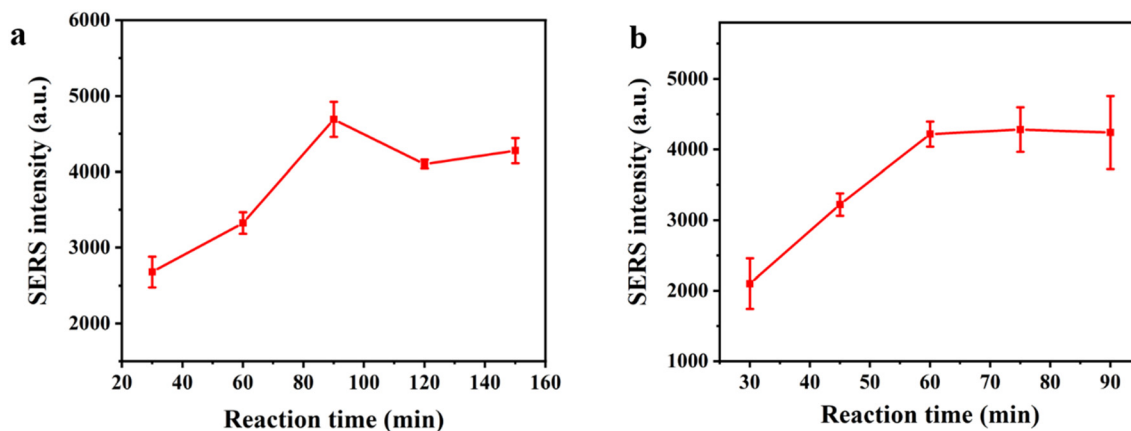


**Fig. 3** (a) Plots of the optimized results for the reaction time of magnetic beads and EXPAR amplification product (trigger DNA) (b) plots of the optimized results for the reaction time of the magnetic bead-trigger complex and Au-Ag mushroom-shaped SERS probes.

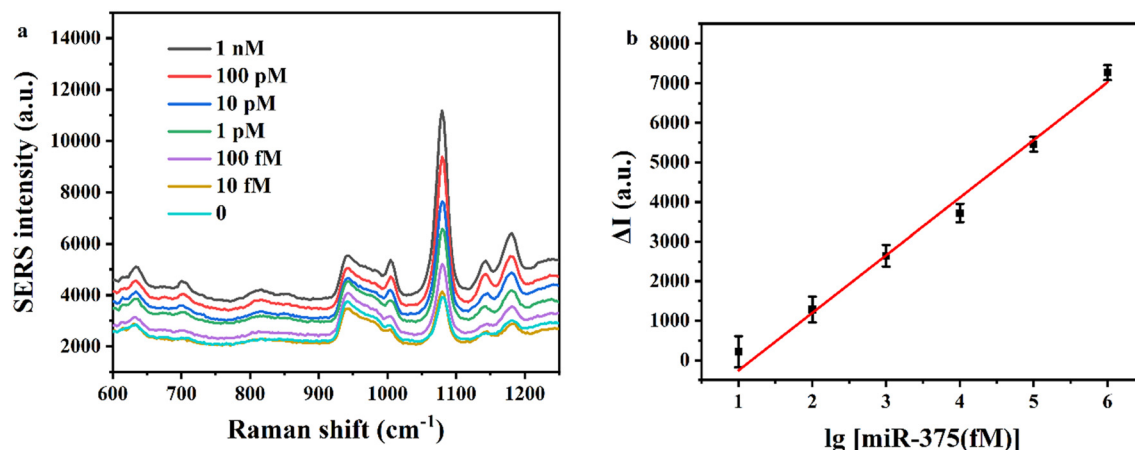


Fig. 4 (a) SERS spectra of different concentrations of miR-375 (concentration range: 10 fM–1 nM), and (b) SERS signal intensity showing a linear relationship with the logarithm of miR-375 concentration, and the error bars indicate the standard deviation measured in three independent experiments.

Lane 3 represents the amplification product with the addition of Vent (exo-) DNA polymerase, dNTPs, and Nt.BstNBI incision enzyme, however, without the addition of template-375, the EXPAR reaction could not occur and no band was produced. Therefore, there were no bands produced. Lanes 4 and 5 are the product bands without the addition of Vent (exo-) DNA polymerase and Nt.BstNBI incision enzyme, respectively, and both are devoid of the target bands produced by the EXPAR reaction. The findings obtained are compatible with the phenomena reported in the literature,<sup>26</sup> showing that the EXPAR reaction was effectively executed.

The feasibility of miR-375 detection assisted with EXPAR and Au–Ag mushroom-shaped SERS probes was also estimated. Raman spectra of the system with and without target miR-375 are shown in Fig. 2(c). With the addition of 0.1 nM miR-375, the spectrum showed the characteristic peaks of the Raman reporter (*p*-ATP), where the peak at 1079 cm<sup>-1</sup> is the strongest peak. The SERS intensity at 1079 cm<sup>-1</sup> increased about 10 times when compared to the absence of miR-375 (Fig. 2(c)), which verified the feasibility of EXPAR and Au–Ag mushroom-shaped SERS probe assisted detection of miRNA. Furthermore, the SERS intensity at 1079 cm<sup>-1</sup> was also chosen as the standard for quantitative detection.

#### 4. Optimization of SERS detection

In order to get the optimum analytical performance for the assay, we optimized the reaction time of the magnetic beads and EXPAR amplification product (trigger DNA), as well as the magnetic bead–trigger complex and Au–Ag mushroom-shaped SERS probe. As shown in Fig. 3a, the SERS intensity steadily rose along with the reaction time of the magnetic beads and trigger DNA, showing that more and more trigger DNA was captured by the magnetic beads. Therefore, 90 min was selected as the capture time. As shown in Fig. 3b, the SERS intensity steadily grew as the reaction time of the

magnetic bead–trigger complex and Au–Ag mushroom-shaped SERS probe was prolonged, and when the reaction time exceeded 60 min, the SERS intensity eventually stabilized. Consequently, the reaction time was selected as 60 min.

#### 5. Detection sensitivity and specificity of the SERS sensor

We investigated the sensitivity of the method using the EXPAR and mushroom-shaped SERS probes under optimized conditions for the detection of various miR-375 concentrations. As seen in Fig. 4a, the SERS intensity steadily increased as the concentration of miR-375 increased from 0 to 1 nM. We found the increment of the SERS intensity ( $\Delta I$ ) ( $\Delta I = I - I_0$ , where  $I$  is the SERS intensity for the detection of various miR-375 concentrations, and  $I_0$  is the SERS intensity without miR-375) was linear to the logarithm of concentration of miR-375 ( $\log[\text{miR-375(fM)}]$ ). The linear regression equation for the relationship between the intensity of the SERS characteristic peak at 1079 cm<sup>-1</sup> and the concentration of miR-375 was  $y = 1455.92 \log C - 1713.28$ , where  $y$  stands for the difference between the SERS intensity of the test object and the blank,  $C$  stands for the concentration of miR-375

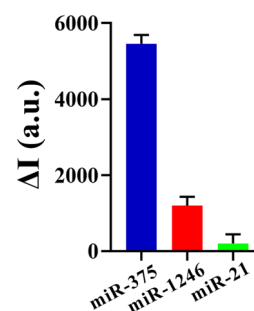
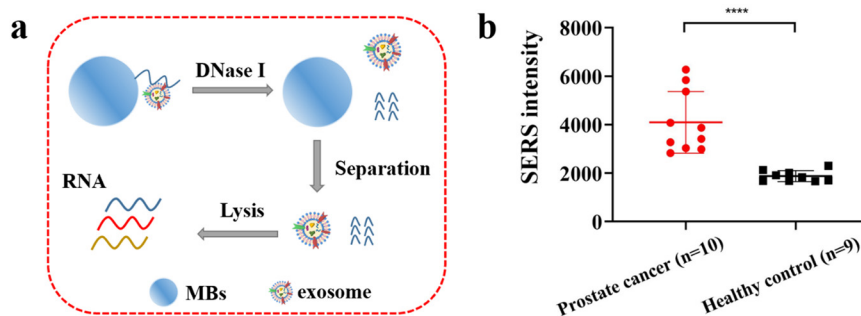


Fig. 5 Specificity study.  $\Delta I$  comparison of three different miRNAs (miR-375, miR-1246 and miR-21, 100 pM); error bars represent the mean standard deviation of the three sets of experiments.





**Fig. 6** Exosome miR-375 assay based on the EXPAR and mushroom-shaped SERS probe for analysis of clinical serum samples. (a) Schematic diagram of exosome release and RNA extraction, and (b) graph of assay results, where the red circular icons indicate serum assay results from prostate cancer patients and black square icons indicate serum assay results from normal subjects (significance analysis using *t*-test: \*\*\*\**p* < 0.0001).

(fM), the correlation coefficient  $R^2$  was 0.9845, and the detection limit was 10 fM (at  $S/N = 3$ ). By contrast, the miRNA assays need an RNA input ranging from 0.025 to 250 ng (approximately 3 fM to 30 pM).<sup>27</sup>

We also tested the interference of two miRNAs (miR-1246 and miR-21) and compared the SERS intensity of these three miRNAs under identical experimental conditions in order to assess the specificity of the approach. Fig. 5 illustrates the differences between miR-375 and the other two interfering miRNAs. These results indicate that the EXPAR and mushroom-shaped SERS probe-based sensor for detecting miRNAs has good specificity.

## 6. Clinical Sample Analysis

The PSMA aptamer modified MBs were employed to capture the exosomes from serum samples and DNase I enzyme was used to shear the PSMA aptamer on the surface of magnetic beads to release exosomes, which were then lysed to obtain the exosomal RNA as shown in Fig. 6(a). And then, the EXPAR and mushroom-shaped SERS probe-based sensor was used for the detection of exosomal miR-375 in clinical serum samples. Fig. 6 shows that the method successfully distinguished between healthy people and patients ( $p < 0.0001$ ) and that the miR-375 assay for PSMA-positive exosomes was accurate for diagnosing prostate cancer. Therefore, it is anticipated that the detection of miR-375 would be utilized to provide an accurate diagnosis of clinical prostate cancer. By gathering more clinical samples and identifying the miR-375 content of PSMA-positive exosomes in the serum of patients with various stages of malignancies, we expect to further investigate and evaluate the viability of this technology for clinical prostate cancer detection and staging in the future.

## Conclusions

We developed an EXPAR and Au-Ag mushroom-shaped SERS probe assisted strategy for the detection of exosomal miR-375 in prostate cancer. The Au-Ag mushroom-shaped SERS probe is formed by DNA that semi-coats silver on the surface of AuNPs and creates a gap at the Au-Ag interface, resulting in

a high SERS signal. With a linear detection range of 10 fM–1 nM for miR-375 and a detection limit of 10 fM, the sensitive detection of miR-375 is accomplished by binding the exposed DNA probe on the opposite side of AuNPs and the EXPAR amplification products triggered by target miRNA. This method has a cheap cost and high detection efficiency, and it reacts at a steady temperature without thermal cycling. More significantly, we discovered that miR-375 of PSMA-positive exosomes in serum is anticipated to be a potential prostate cancer diagnostic by examination of clinical data.

## Conflicts of interest

There are no conflicts to declare.

## Acknowledgements

This work was jointly supported by the National Natural Science Foundation of China (22274028, 22174022, and 22127806), the Shanghai Natural Science Foundation (20ZR1403000), and the Shanghai Science and Technology Innovation Action Plan (20392001900).

## References

1. L. He and G. J. Hannon, MicroRNAs: Small RNAs with a Big Role in Gene Regulation, *Nat. Rev. Genet.*, 2004, 5(7), 522–531.
2. D. P. Bartel, MicroRNAs: Genomics, Biogenesis, Mechanism, and Function, *Cell*, 2004, 116(2), 281–297.
3. V. Ambros, The Functions of Animal MicroRNAs, *Nature*, 2004, 431(7006), 350–355.
4. Q. Feng, W. Fan, W. Ren and C. Liu, Recent Advances in Exosome Analysis Assisted by Functional Nucleic Acid-Based Signal Amplification Technologies, *TrAC, Trends Anal. Chem.*, 2022, 116549.
5. K. M. Kim, K. Abdelmohsen, M. Mustapic, D. Kapogiannis and M. Gorospe, RNA in Extracellular Vesicles, *Wiley Interdiscip. Rev. RNA*, 2017, 8(4), e1413.
6. L. Zhu, X. Liu, W. Pu and Y. Peng, TRNA-Derived Small Non-Coding RNAs in Human Disease, *Cancer Lett.*, 2018, 419, 1–7.





- 7 K. Yang, Q. Zhou, B. Qiao, B. Shao, S. Hu, G. Wang, W. Yuan and Z. Sun, Exosome-Derived Noncoding RNAs: Function, Mechanism and Application in Tumour Angiogenesis, *Mol. Ther.–Nucleic Acids*, 2022, **27**, 983–997.
- 8 A. Yokoi, Y. Yoshioka, A. Hirakawa, Y. Yamamoto, M. Ishikawa, S. Ikeda, T. Kato, K. Niimi, H. Kajiyama and F. Kikkawa, A Combination of Circulating MiRNAs for the Early Detection of Ovarian Cancer, *Oncotarget*, 2017, **8**(52), 89811.
- 9 K. Boriachek, M. N. Islam, A. Möller, C. Salomon, N.-T. Nguyen, M. S. A. Hossain, Y. Yamauchi and M. J. Shiddiky, Biological Functions and Current Advances in Isolation and Detection Strategies for Exosome Nanovesicles, *Small*, 2018, **14**(6), 1702153.
- 10 X. Huang, T. Yuan, M. Liang, M. Du, S. Xia, R. Dittmar, D. Wang, W. See, B. A. Costello and F. Quevedo, Exosomal MiR-1290 and MiR-375 as Prognostic Markers in Castration-Resistant Prostate Cancer, *Eur. Urol.*, 2015, **67**(1), 33–41.
- 11 J. Zhao, C. Liu, Y. Li, Y. Ma, J. Deng, L. Li and J. Sun, Thermophoretic Detection of Exosomal MicroRNAs by Nanoflakes, *J. Am. Chem. Soc.*, 2020, **142**(11), 4996–5001.
- 12 H. Yan, Y. Wen, Z. Tian, N. Hart, S. Han, S. Hughes and Y. Zeng, A Highly Sensitive and Robust One-Pot Assay for the Detection of MicroRNAs, *Nat. Biomed. Eng.*, 2023, 1–2.
- 13 M. S. Reid, X. C. Le and H. Zhang, Exponential Isothermal Amplification of Nucleic Acids and Assays for Proteins, Cells, Small Molecules, and Enzyme Activities: An EXPAR Example, *Angew. Chem., Int. Ed.*, 2018, **57**(37), 11856–11866.
- 14 R.-D. Li, B.-C. Yin and B.-C. Ye, Ultrasensitive, Colorimetric Detection of MicroRNAs Based on Isothermal Exponential Amplification Reaction-Assisted Gold Nanoparticle Amplification, *Biosens. Bioelectron.*, 2016, **86**, 1011–1016.
- 15 J. Nie, D.-W. Zhang, C. Tie, Y.-L. Zhou and X.-X. Zhang, G-Quadruplex Based Two-Stage Isothermal Exponential Amplification Reaction for Label-Free DNA Colorimetric Detection, *Biosens. Bioelectron.*, 2014, **56**, 237–242.
- 16 J. Qian, Q. Zhang, M. Liu, Y. Wang and M. Lu, A Portable System for Isothermal Amplification and Detection of Exosomal MicroRNAs, *Biosens. Bioelectron.*, 2022, **196**, 113707.
- 17 J. U. Lee, W. H. Kim, H. S. Lee, K. H. Park and S. J. Sim, Quantitative and Specific Detection of Exosomal MiRNAs for Accurate Diagnosis of Breast Cancer Using a Surface-Enhanced Raman Scattering Sensor Based on Plasmonic Head-Flocked Gold Nanopillars, *Small*, 2019, **15**(17), 1804968.
- 18 T. Kang, J. Zhu, X. Luo, W. Jia, P. Wu and C. Cai, Controlled Self-Assembly of a Close-Packed Gold Octahedra Array for SERS Sensing Exosomal MicroRNAs, *Anal. Chem.*, 2021, **93**(4), 2519–2526.
- 19 M. Pellarin, J. Ramade, J. M. Rye, C. Bonnet, M. Broyer, M.-A. Lebeault, J. Lermé, S. Marguet, J. R. G. Navarro and E. Cottancin, Fano Transparency in Rounded Nanocube Dimers Induced by Gap Plasmon Coupling, *ACS Nano*, 2016, **10**(12), 11266–11279.
- 20 J.-M. Kim, J. Kim, K. Choi and J.-M. Nam, Plasmonic Dual-Gap Nanodumbbells for Label-Free On-Particle Raman DNA Assays, *Adv. Mater.*, 2023, **35**(15), 2208250.
- 21 J. Su, D. Wang, L. Nörbel, J. Shen, Z. Zhao, Y. Dou, T. Peng, J. Shi, S. Mathur and C. Fan, Multicolor Gold–Silver Nano-Mushrooms as Ready-to-Use SERS Probes for Ultrasensitive and Multiplex DNA/MiRNA Detection, *Anal. Chem.*, 2017, **89**(4), 2531–2538.
- 22 D. Jin, F. Yang, Y. Zhang, L. Liu, Y. Zhou, F. Wang and G.-J. Zhang, ExoAPP: Exosome-Oriented, Aptamer Nanoprobe-Enabled Surface Proteins Profiling and Detection, *Anal. Chem.*, 2018, **90**(24), 14402–14411.
- 23 K. C. Grabar, R. G. Freeman, M. B. Hommer and M. J. Natan, Preparation and Characterization of Au Colloid Monolayers, *Anal. Chem.*, 1995, **67**(4), 735–743.
- 24 Z. Huang, Q. Lin, B. Yang, X. Ye, H. Chen, W. Weng and J. Kong, Cascade Signal Amplification for Sensitive Detection of Exosomes by Integrating Tyramide and Surface-Initiated Enzymatic Polymerization, *Chem. Commun.*, 2020, **56**(84), 12793–12796.
- 25 J. Shen, J. Su, J. Yan, B. Zhao, D. Wang, S. Wang, K. Li, M. Liu, Y. He and S. Mathur, Bimetallic Nano-Mushrooms with DNA-Mediated Interior Nanogaps for High-Efficiency SERS Signal Amplification, *Nano Res.*, 2015, **8**, 731–742.
- 26 Y. Wang, X. Zhao, M. Zhang, X. Sun, J. Bai, Y. Peng, S. Li, D. Han, S. Ren, J. Wang, T. Han, Y. Gao, B. Ning and Z. Gao, A Fluorescent Amplification Strategy for High-Sensitive Detection of 17  $\beta$ -Estradiol Based on EXPAR and HCR, *Anal. Chim. Acta*, 2020, **1116**, 1–8.
- 27 C. Chen, D. A. Ridzon, A. J. Broomer, Z. Zhou, D. H. Lee, J. T. Nguyen, M. Barbisin, N. L. Xu, V. R. Mahuvakar, M. R. Andersen, K. Q. Lao, K. J. Livak and K. J. Guegler, Real-Time Quantification of MicroRNAs by Stem-Loop RT-PCR, *Nucleic Acids Res.*, 2005, **33**(20), e179.

